This is a preprint version of the article. See http://dx.doi.org/10.1109/TMECH.2014.2315762 for the publishers version.
L. Palmer, E. Diller, and R. Quinn, "Distributed Inward Gripping: A Gravity-Independent Attachement Strategy for Complex Climbing Maneuvers," *IEEE Transactions on Mechatronics,* vol. 20, no. 2, pp. 631-640.

Distributed Inward Gripping: A Gravity-Independent Attachment Strategy for Complex Climbing Maneuvers

Abstract

The biologically-inspired strategy of Distributed Inward Gripping (DIG) is presented in this work as a method for foot attachment and adhesion during gravity-independent climbing. As observed in nature, this strategy enables climbing animals to maneuver rapidly on surfaces in any orientation with respect to gravity, and does not require significant energy expenditure for attachment or detachment. DIG is implemented on a hexapod, DIGbot, which is fully contained with power and control onboard. Utilizing DIG, the robot is able to climb and make turns on both vertical and inverted mesh screen using cockroach-inspired prehensile claws. The spacing in the mesh screen requires each foot to perform a local search for an adequate foothold, which mimics what has been observed in climbing insects. The principle of distributed inward gripping is also suited for use with micro-spine arrays and gecko-inspired dry adhesive pads being developed in other laboratories.

I. Introduction

The ability to scale vertical surfaces and walk inverted on ceilings greatly extends the mobility of insects and many other small animals. Robots that could achieve similarly rapid and robust locomotion in any orientation with respect to gravity have potential in applications including military reconnaissance, time-critical search and rescue in unstructured environments, planetary exploration and spacecraft maintenance in reduced-gravity environments.

Climbing robotic systems have been developed for use in other applications, such as tank crack inspection (Choi et al. 2004), window cleaning (Zhang et al. 2006), pipe inspection (Murats Tur 2007, Tavakoli et al. 2010) and welding on ferromagnetic surfaces (Gonzalez de Santos et al. 2000). These and other climbing systems employ vacuum cups with and without suction, magnets and tape. While these systems perform well on certain surfaces or for brief tasks, they have not been shown to climb on a variety of surfaces over an extended period of time.

Humans and many animals use versatile multi-jointed legs to climb vertically on a variety of surfaces, and can utilize these legs to walk over discontinuous terrain, run over rough terrain and jump onto or over obstacles. Greater than the advantages that multi-jointed legs provide during each individual mode of locomotion is their ability for multi-modal performance. This is the greatest incentive to develop biomorphic legged systems, which seek to increasingly mimic the structure and control systems observed in animals in order to ultimately achieve the full functionality as seen by animals in nature. The goal of this work is to investigate and demonstrate a biologically-inspired climbing approach on a biomorphic system. DIGbot, shown in Figure 1, is used to investigate the bio-inspired climbing strategy, Distributed Inward Gripping (DIG).

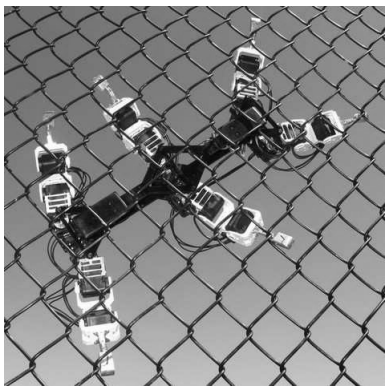

Figure 1. The Distributed Inward Gripping (DIG) strategy is tested on DIGbot, an 18 degree-of-freedom hexapod with onboard power and control system. Here is it shown passively gripping a vertical chain link fence with 6 *cm* spacing.

The primary aspect of climbing investigated in this work is an attachment strategy used to adhere robotic feet to a climbing surface during movement in any orientation with respect to gravity. Attachment mechanisms for gravity-independent climbing must support forces normal to the surface that hold the system to the surface as well as shear forces tangential to the surface that move the body and prevent the system from sliding down the surface. A directional attachment device engages with the surface to provide these forces when pulled tangentially along the surface in a single direction, and disengages with the surface when the tangential pulling force is released. While engaged, a directional attachment mechanism can produce shear forces for motion in multiple directions and animals can often manipulate articulated legs to dictate the direction for attachment and detachment.

The tangential force used to maintain engagement can also result in unwanted motion if unopposed. Some animals such as cats rely on the downward pull of gravity to oppose the tangential attachment force, which in some cases limits the direction of climb available to these animals. Cats normally do not climb down trees head first.

Directional attachment is used by cockroaches (Goldman et al. 2006), geckos (Autumn et al. 2006) and other animals, each with different attachment mechanisms and adhesive materials. Figure 2 shows a set of cockroach claws and spines. The claw engages with the surface when pulled tangentially along the surface in the attachment direction, which for the orientation shown in Figure 2 is to the left, and can then produce normal attachment forces and shear walking forces. Detachment is energetically inexpensive and very rapid because the claw only needs to be relaxed in the opposite tangential direction to disengage from the surface. Kim et al. describe this process as controlling adhesion by controlling shear (Kim et al. 2007).

Figure 2. Cockroach claws and spines. When engaged with a surface, the claw resists motion and generates ground reaction forces when pulled in one direction (left, as shown) and allows for motion in the opposite direction (Wei 2004).

Robotics systems have been developed using directional attachment materials and mechanisms to climb vertically. The RiSE (Robots in Scansorial Environments) project produced valuable insights into optimized leg mechanisms for climbing diverse terrains (Spenko et al. 2006). As part of the RiSE project, the Spinybot robot (Asbeck et al., 2006) detailed how a passive structure in shear can engage with a surface. It was the first to use passive compliance built into each spine of a multi-spine foot. The RiSE robot can climb vertically up trees, carpeted surfaces and stucco, although different feet are required for each surface. The LIBRA robot climbs up pegboard-like surfaces using articulated legs, and has produced insight into force distribution and planning while climbing (Madhani and Dubowsky, 1997; Bevly et al., 2000). The LEMUR class of robots has also achieved steep terrain access by attaching to footholds much like human climbers (Bretl et al. 2004). The DynoClimber (Lynch et al., 2012) also uses passive, directional spines to rapidly climb up near-vertical surfaces. The speed at which this robot climbs displays one of the before-mentioned advantages of directional attachment mechanisms – rapid attachment and detachment.

Climbing Mini-Whegs climbed vertical glass walls using a dry adhesive by attaching and detaching its feet similar to an insect (Daltorio et al. 2009). It rolled its feet onto the surface and peeled them off for rapid attachment and detachment. Stickybot, which can climb vertically up smooth glass, utilizes gecko-inspired feet which hyperextend in order to peel dry directional adhesive pads (Kim et al. 2008). Dry adhesives that are directional in operation are being developed by Sitti (Murphy and Sitti 2007, Murphy et al. 2008), Fearing (Lee et al. 2009), Autumn (Autumn et al. 2006), Gorb (Gorb et al. 2007) and others, and will ultimately lead to lightweight, low-energy, and robust attachment materials for robotic climbing.

Distributed Inward Gripping (DIG), used by insects (Niederegger and Gorb 2003), is a variation of directional attachment which dictates that legs pull inward towards the body during attachment. Directing the forces inward ensures that the shear forces necessary to engage the attachment mechanisms work in opposition to each other. Niederegger and Gorb (2003) showed that an insect could attach and hold itself inverted with just two contralateral legs. Directing the attachment forces to oppose one another rather than relying on gravity opposition allows the system to walk on surfaces in any orientation with respect to gravity. Directional attachment mechanisms utilized in this manner are also suitable for climbing in the micro gravity environments of space applications. In this work, legs are directed to pull inward at an angle perpendicular to an imaginary bisector that divides the body into left and right halves. This direction was chosen to decouple the attachment forces from walking forces in the fore and aft directions.

DIG was previously shown viable for gravity-independent walking in a single direction (no turns) on mesh screens (Palmer et al. 2009).The algorithm is now applied to an 18 degree-of-freedom (DOF) hexapod, DIGbot, which is designed for more complex maneuvers such as sharp turns and transitions between orthogonal surfaces. DIGbot can walk up, down, left and right on vertical and inverted surfaces without changing its attachment/detachment protocol or walking strategy.

The surface primarily used for this work is mesh screen. Screen was selected over Velcro and other more homogeneous surfaces because the mesh spacing (8.5 mm) forces each foot to seek tangentially inward for a suitable foothold at each step. This local search mimics what has been observed in climbing animals such as locusts (Pearson and Franklin 1984), cockroaches (Tryba and Ritzmann 2000, Delcomyn 1997) and stick insects (Bassler 1993), and is suitable to attach claws or other directional grippers. DIGbot uses a single claw on each foot that works similarly to cockroach claws described above. The inward gripping strategy being developed in this paper is also applicable to other systems that utilize the previously-mentioned dry adhesive pads or micro-spine arrays at the foot.

During static attachment, distributed inward gripping replicates the three-finger force-closure problem (Nguyen, 1988; Ponce and Faverjon, 1995) with the screen as a 2-dimensional object. The mesh grid, however, ensures the existence of an equilibrium grasp, and the grasp positions can be computed based upon other considerations such as achievement of optimal step lengths. The main deviation from force closure research lies in the fact that here the force vectors on the grasped object do not remain constant during the step because of changing robot joint positions.

The purpose of the work presented in this paper is the investigation of Distributed Inward Gripping as a viable strategy for bio-inspired leg adhesion during complex robotic maneuvers on vertical and inverted surfaces. Among other things, this involves the kinematic design of an inward pulling leg, force feedback to detect engagement with the terrain and the development of compliant tarsi to maintain the inward gripping direction while the robot moves without electronic feedback. The DIGbot project differs in scope from the RISE and other projects, in which robots have climbed a variety of surfaces using several degrees-of-freedom legs. The goal of this project is to explore insect-inspired DIG in a climbing robot. DIGbot's three DOF legs are necessary to allow for a wide range of testing configurations in which the robot is required to achieve inward gripping for stable climbing.

Distributed Inward Gripping is discussed next in further detail, followed by a description of DIGbot, the hexapod used to investigate the gripping strategy. Control aspects of DIG are detailed and results are shown and discussed. The paper ends with a summary of the work and the next steps for this project.

II. Distributed Inward Gripping

This work seeks to further investigate the biologically-inspired Distributed Inward Gripping (DIG) attachment strategy through its application on DIGbot, shown in Fig. 1. DIG uses directional

attachment mechanisms by directing laterally-opposing legs to pull inward toward the center line of the body. DIG is tested in the tripod gait, but can be extended to additional gaits. Figure 3 shows the lateral inward direction, through which legs of the attaching tripod pull to engage the claws. To lift from the surface, the legs of the detaching tripod relax their inward pull.

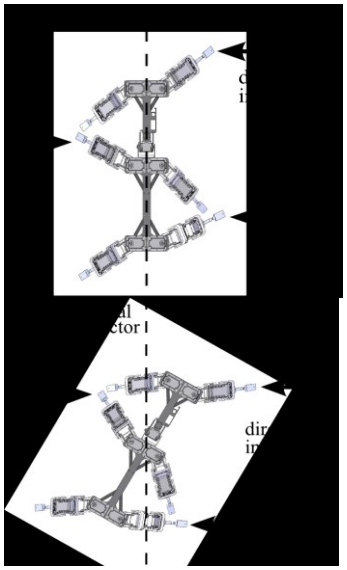

(a) (b)

Figure 3. DIGbot moving through a turn. The direction of inward pull remains unchanged during a step. (a) The body and direction of the inward pull at the beginning of a step. (b) The body position and inward gripping direction after a stationary turn.

The dependence on gravity to engage attachment mechanisms is avoided by directing opposing legs to pull laterally inward. The same kinematic gripping motions will engage the claw and maintain adhesion regardless of the robot's orientation with respect to gravity. The direction of inward pull remains constant with respect to the screen throughout the step, regardless of how the body changes orientation. Figure 3 shows the start and end body position of a step, during which the body makes a stationary turn; the legs are directed to pull laterally toward the initial bisector. A foot with passive compliance similar to insect tarsi is used to passively maintain this initial inward pulling direction without electronic feedback.

Because the inward pulling direction remains constant with respect to the surface through the step, only one direction of terrain support must be tested at contact. This is highly useful for complex surfaces on which the terrain only provides a solid foothold in limited directions. Maintaining the initial direction of pull will also be necessary to extend DIG for use with animal-inspired dry adhesive pads.

III. DIGbot

The body of DIGbot measures 36 cm between the fore and hind hip locations and has a width of 8 cm between contralateral hips. The leg joints are powered by Dynamixel servomotors (Robotis, Inc.), which were chosen over standard DC motors, pneumatic cylinders or other options because of their versatility. These serially-controlled servomotors have communication capabilities including load, velocity and position feedback, and can enforce a user-set torque limit. Custom DIGbot parts are machined from 6061 aluminum and Delrin.

The total mass of DIGbot is approximately 2.2 kg, including onboard power and microcontroller. Control of DIGbot is performed onboard using a TS-7260 single-board computer (SBC) from Technologic Systems, Inc., which runs on a 40MHz EP9302 processor from Cirrus and has a typical power consumption of 2W. The masses of the individual DIGbot components are shown in Table 1. The body frame is made of four custom Delrin brackets held together by a central block, resulting in significant twist compliance. The six hip motors bolt directly to these frame pieces. The microcontroller mounting plates are an extension of the frame, which can deflect a large amount on impact without damaging the board.

Component	Mass (g)	Quantity
Servo battery	190	1
Microcontroller battery	76	1
AX-12 servo	56	19
Mounting brackets per leg	37	6
Body frame	100	1
Serial cable	4	19
Foot	12	6
Microcontroller	226	1
Fasteners	130	1
Total	2231	

Table 1. DIGbot mass parameters.

The spacing and alignment of DIGbot hip locations were determined by optimizing the achievable motion of a single step. Step length is limited due to interference between adjacent ipsilateral legs. Lengthening the fore-aft spacing between hip locations reduces this problem and allows for longer step length, but reduces the achievable turn per step. A compromise was found that allowed DIGbot to turn at angles comparable to cockroaches (Jindrich and Full 1999). Results shown later confirm this.

All six legs are identical to simplify design, construction, control and maintenance. The three servo motors on each leg control fore-aft swing, levation and depression. The fore-aft servos, controlling angle ϕ_1 in Figure 4, have a sweep range of approximately 130 *degrees*. The remaining two servos levate and depress the leg while also lengthening the shortening the radial distance between the hip and foot. Leg dimensions are shown in Figure 5.

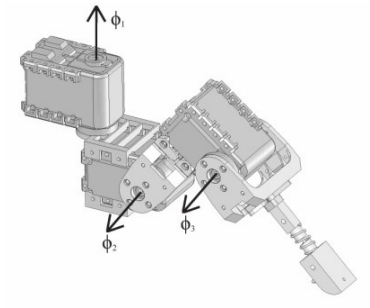

Figure 4. Leg assembly. Each hexapod leg is identical and has three actuated degrees of freedom, with motion along axes ϕ_1, ϕ_2 and ϕ_3.

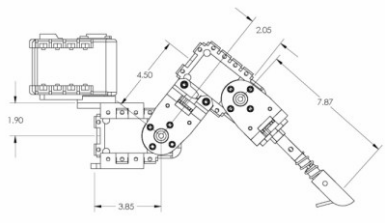

Figure 5. Link lengths for a single leg, with dimensions in cm.

Ankle and foot designs are critical elements for legged climbing systems. DIGbot achieves adhesive (tangent to the substrate) forces through the use of pointed claws on each of its feet. This allows for simple yet robust attachment on screen mesh. Claws were chosen because of their potential for stable, directional gripping necessary to investigate and demonstrate the DIG principle.

The tarsus and foot assembly, shown in Figure 6, consists of a stainless steel claw embedded in an aluminum foot which is attached by a spring to the rest of the leg. A braided steel cable, held with set screws, runs through the middle of the assembly and bears the axial load of the assembly. The aluminum foot geometry is such that the face of the foot is always presented prone to the substrate for any leg approach angle. This allows the claw length and orientation to be optimized for a nominal foot-substrate angle.

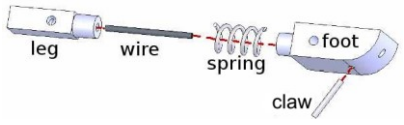

Figure 6. Exploded foot assembly. The foot design allows for passive claw reorientation using a sprung tarsus joint.

Figure 7 shows the claw engaged in the mesh screen. See also Figure 9 for more views. The mesh is made from nickel-plated steel wire and has a wire spacing of 8.5 mm.

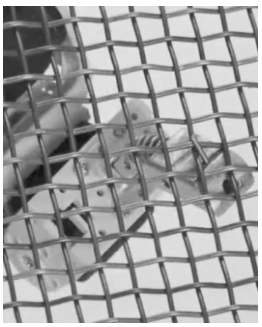

Figure 7. DIGbot claw engaged with the mesh screen.

Directional attachment operates under the condition that the foot only produces a gripping force when pulled in a single direction, and DIG dictates that force be in opposition to contralateral legs. After being depressed to the surface, the foot is pulled tangentially inward, causing the claw to seek the inward wire in the mesh and develop a gripping force. During a step, the leg angle changes with respect to the inward gripping direction. In order to properly maintain the desired inward gripping direction, the axis of the foot must be kept stationary during the step. Figure 8 shows the deflection of a compliant cockroach tarsus (foot) during a forward step. This deflection enables the attachment mechanism to maintain its initial orientation with the substrate throughout the step.

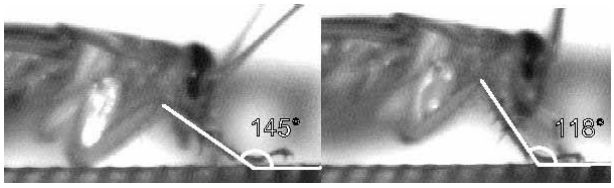

Figure 8. A cockroach moving through a step. The tarsus consists of multiple segments connected with spring loaded (resilin) joints with claws at the distal end. A muscle in the tibia flexes the claws via a tendon and the claws extend via the passive springs. This image originally produced in (Frazier 1999).

A passive tarsus has been incorporated on DIGbot to replicate the functionality of the cockroach tarsus. As described above, Spinybot's feet also have passive compliance (Asbeck et al., 2006), but its feet were designed for climbing vertical walls in the forward direction. DIGbot's climbing required compliance in more than one degree of freedom like the cockoach. Figure 9 shows the achievable motion of a DIGbot tarsus as it maintains the desired gripping direction, highlighted by the arrow in each subfigure. Subfigure (a) indicates rotation through the tarsus *vertical* angle to two typical positions, and subfigure (b) indicates rotation through the tarsus *swing* angle. When the claw is removed from the screen at the end of stance, the foot springs back to its nominal straight position. This tarsus design results in proper inward gripping during the entire stance phase without the use of electronic feedback or an actuated tarsus joint.

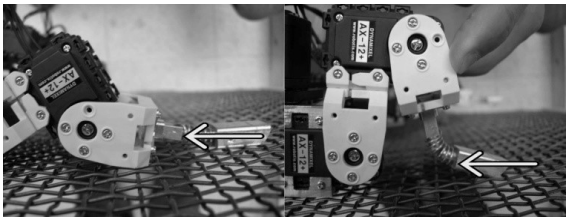

(a) Bending on vertical axis

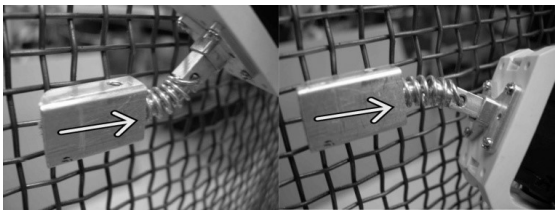

(b) Bending on swing axis

Figure 9. DIGbot compliant tarsus. As the body moves through a step, the angle of the leg changes with respect to the desired inward force, and the claw rotates about its pivot to maintain the desired inward gripping direction. The arrow shows the direction of inward gripping in each subfigure. Subfigure (a) shows rotation through the tarsus vertical angle to two positions encountered during walking and turning. Subfigure (b) shows the rotation through the tarsus swing angle.

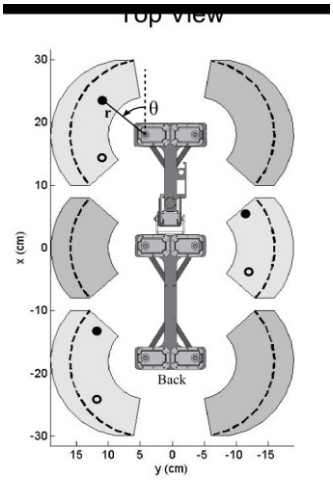

Figure 10. The allowable surface workspace for each leg when the undercarriage of the body lies against the substrate. For clarity, the legs are not shown. The darkened circles represent the optimized starting foot positions (after inward gripping) with respect to the body for a straight step, and the open circles represent the foot placements at the end of the step. Each workspace is divided into inner and outer subspaces by the dashed line. The outer subspace represents 3 cm of lateral space for the inward gripping motion, leaving only the inner subspace available for the stepping motion, which occurs after gripping.

IV. Stepping Algorithm

For legged systems on a variety of substrates, the control of individual legs involves cycling between swing, engagement, stance, and disengagement movements. Swing normally involves protracting the foot forward to the desired location for the next touchdown. Engagement consists of moving the foot toward the surface and establishing a good foothold capable of supporting the anticipated load through stance.

The desired foot location at touchdown is computed through a brute force search of each leg's workspace to minimize the necessary joint motions for the desired walking trajectories. Using the optimal touchdown locations, DIGbot can take a forward step of up to 25% of its body length and make a turn of up to 32 degrees. Figure 10 shows the allowable surface workspace for each leg when the undercarriage of the body lies against the substrate.

Each workspace is divided into inner and outer subspaces by the dashed line. The outer subspace contains an additional 3 *cm* of lateral space for the inward gripping motion, leaving only the inner subspace available for the stepping motion, which occurs after gripping. Therefore, the brute force search is constrained to the inner subspace in its search for touchdown and liftoff positions. The darkened small circles in Figure 10 represent the optimized starting foot positions (after inward gripping) with respect to the body for a straight step, and the open circles represent the foot placements at the end of the step. The foot positions are parameterized by cylindrical coordinates (r, Θ, h) with respect to each hip. The body height, h, is not shown in this figure, but is kept constant at 3.8 cm to keep the body undercarriage against the surface.

Attachment

DIGbot is tested on a manually-rotatable screen, illustrated in Figure 11**Error! Reference source not found.**. The screen angle is measured from vertical and can be adjusted for climbing in any orientation with respect to gravity.

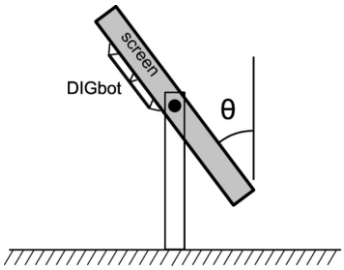

Figure 11. Side view of test screen illustration. DIGbot is tested on a manually-rotatable screen, whose angle is described with respect to the vertical axis.

A free-body diagram of DIGbot in static climbing is shown in Figure 12. By summing moments about two different foot attachment points (blue dots), the normal force supported by each foot can be calculated. Forces tangent to the mesh substrate are not shown because they do not affect this calculation. Furthermore, the tangential force supported by each foot is not calculated because attachment shear failure is never observed in practice because the mesh and claw are both stiff.

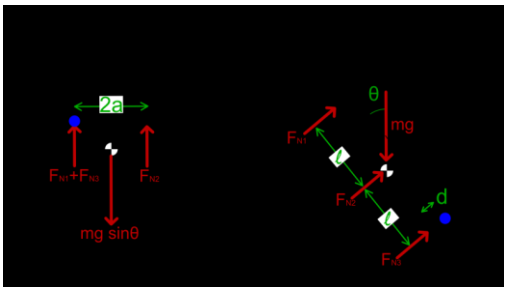

Figure 12. Free body diagram of DIGbot on ground/screen.

Summing moments about the blue dot in the front view gives

$$F_{N2}(2a) = mg\sin\theta(a) \quad (1)$$

and about the blue dot in the side view

$$F_{N2}(l) + F_{N1}(2l) - mg\cos\theta(d) - mg\sin\theta(l) = 0 \quad (2)$$

Solving for F_{N1}:

$$\frac{F_{N1}}{mg} = \frac{\cos\theta(d) + \sin\theta(l) - \frac{1}{2}\sin\theta(l)}{2l} \quad (3)$$

This function gives the body weight-normalized normal force supported by a front foot, which is the most common point of failure, as a function of screen angle θ. Foot gripping failure is noted by the slip of the foot spine off of the mesh screen, which indicates that not enough inward force has been generated. Another possible cause for slipping could be deformation of the mesh screen, but this was not observed even during solid attachment with maximum inward force being delivered. Further discussion of failures appears in the Results Section.

Figure 13 shows this function plotted with experimental data taken over a range of inverted screen angles. Experiments were run with robot masses of 1880 *g*, 2100 *g* and 2720 *g* by removing the batteries and hanging a payload from the center of mass. For each test, steps were taken with decreasing initial inward gripping force until climbing failure occurred. Each data point represents the smallest gripping force with which three consecutive steps were taken at each mass and screen angle. The minimum DIG force is simply a threshold value during the initial foot attachment and does not include measurements of the DIG force during the movement portion of stance. The gripping force for each leg is computed using the inverse of the Jacobian transpose and quasistatic current feedback from each of the servos to approximate joint torque, τ, using the equation,

$$F = (J^T)^{-1}\tau \quad (4)$$

where F is a 3x1 vector of the foot force applied by the leg and J is the Jacobian of a leg.

In Figure 13, the vertical axis is a non-dimensional ratio of force divided by DIGbot weight, allowing data to be compared across robot masses. A quadratic line is fit to each mass data set and the theoretical normal force on the fore foot in contact (Eq. 3) is plotted as the dashed line. The normal force is seen to be roughly proportional to the required inward gripping force. In addition, it can be seen that in the worst-case scenario (approximately 75 *deg*), the inward gripping force must be at least half the weight of the robot to ensure successful climbing.

Equation 3 can now be used as a guideline for computation of an approximate attachment force required for climbing. If the robot mass and screen angle are known, this information can be used to select only the minimum required gripping force, resulting in less harm to fragile substrates as well as significant energy savings, as opposed to using the maximum gripping force.

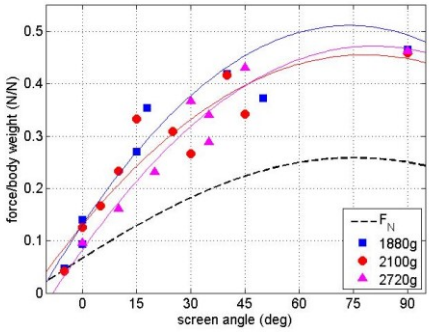

Figure 13. Experimental results showing the minimum gripping force as a function of screen angle. Force is shown as a non-dimensional ratio of the gripping force divided by the body weight. Each data point represents the smallest gripping force for which three consecutive steps were taken at each mass and screen angle. A quadratic line is fit to each body mass data set and the theoretical normal force on the fore foot in contact (eq. 3) is plotted as the dashed line. These data show that the inward gripping force must be at least half of the body weight to ensure successful gripping at extreme screen angles.

The DIG force for all three legs during the attachment phase is presented in Figure 14. The attachment phase shown is much slower than a normal attachment so that force data can be gathered with sufficient temporal resolution. Again, load data is computed using Eq. 4 and is filtered in real time. In real operation, the inward gripping phase takes less than a tenth of a second for each grip attempt. The *verify* dots signify the times when the DIG force is measured and compared with the threshold value (0.55 times robot weight in this example). During normal operation, the gripping force is only measured at the *verify* points and not during the entire process as shown here. The figure shows that at the first grip attempt

at 2.7 seconds, only the middle leg has surpassed the DIG threshold. As a result, the middle leg is kept stationary during the remainder of the gripping process. The fore and aft feet did not achieve the threshold DIG force after the first grip, and must reset. The reset process can be seen as the DIG force going to zero at 3.0 seconds. The second grip, completed at 5.8 seconds, is successful for the aft leg, but not for the fore leg. The fore leg only achieves the proper grip on attempt three at 8.8 seconds. At this point, all three legs forming a tripod have achieved satisfactory grip and DIGbot removes the alternate tripod from the screen in preparation for stance motion. This particular attachment phase with multiple misses is atypical and was chosen to help discuss the full algorithm in a worst case scenario and at slow speed.

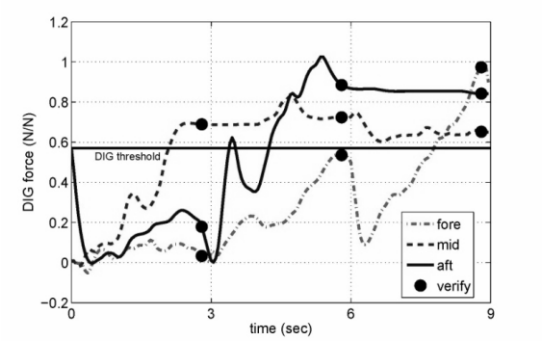

Figure 14. The inward gripping forces during an attachment phase. The attachment phase shown is much slower than a normal attachment so that force data can be gathered with sufficient bandwidth. In real operation, the inward gripping phase takes less than a tenth of a second for each grip. Also, the gripping force is only measured at the instances labeled 'verify' and not during the entire process as shown here. At the first attempt to verify, only the middle leg has attached properly. At the second attempt, the middle and aft leg have attached. Successful gripping for the tripod is not realized until all three legs achieve an inward force above the desired threshold, which occurs at the third attempt to verify.

After the attaching tripod has fully engaged its claws and the detaching tripod has disengaged, the stance legs are actuated to move the body through a desired trajectory.

Detachment begins by reducing power to the detaching legs, which reduces the inward gripping force. The claws are then lifted normally from the surface. The tarsus joint compliance reduces the likelihood that the claws catch on the mesh screen during detachment.

V. Results

Figure 15 shows the swing angle (ϕ_1 in Figure 4) and leg length for the front left leg during a straight step. The desired leg angle and length result in a trapezoidal velocity profile of the body during the step. The actual leg angle and length for climbing vertically and walking on horizontal ground are shown. When walking on horizontal ground, body motion is orthogonal to the force of gravity and almost no error exists in the final leg positions. However, when climbing vertically, steady state errors exist in the servo motors as the pull of gravity now opposes the desired motion. Positional errors also arise due to the inward gripping strategy. The maximum inward search distance is set to be just larger than the screen spacing, which is known and fixed, but the robot has no knowledge of where the claw is relative to the wire when the inward search begins. After inward gripping ends, the position of the foot with respect to the body is also unknown and not recomputed. This is a limitation of the current algorithm and can be addressed in future versions. The errors shown are representative of a typical step and contribute to errors in body motion, which are shown later.

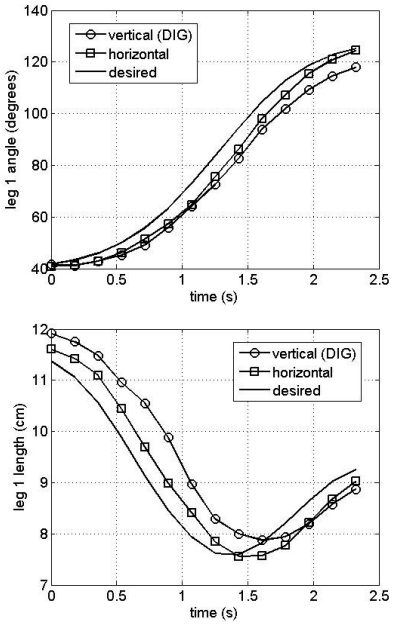

Figure 15. Leg angle and length of leg 1 (left, fore leg) while the body executes a straight step on a vertical and horizontal surface. Less error occurs when walking on the horizontal surface, as the servos do not have to support the weight of the body.

During stance, the relative angle of the legs with respect to the screen changes. Figure 16 shows the tarsus bend computed from the leg length and angle during a straight step and stationary turn, respectively. The vertical angle of the hind tarsus (shown in Figure 9a) bends approximately 14 *degrees* during a straight step. The fore, mid and hind tarsus swing angles each undergo approximately 40 *degrees* of rotation as each leg undergoes the same trajectory for the straight walk. For the turn, the fore and hind tarsi bend approximately 17.5 *degrees* on the vertical axis and approximately 50 *degrees* on the swing axis. Despite these large angle ranges, the passive compliance in the tarsus allows the leg to maintain lateral inward gripping without electronic feedback.

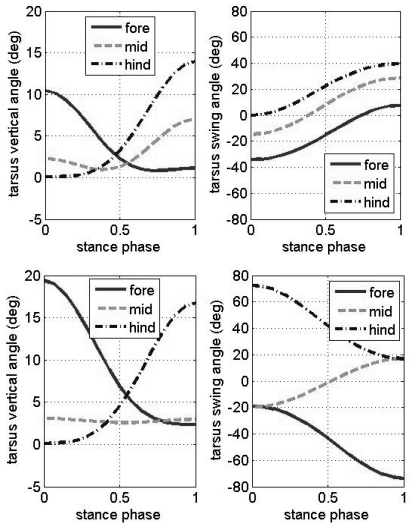

(a) Straight step (b) Turn

Figure 16. Calculated tarsus angles measured from the straight orientation for a stationary turn. The angles are shown for all three tripod legs during a single stance phase. The left subplot shows the vertical angle which is related to the radial distance from hip to foot. The right subplot shows the tarsus swing angle which varies as the leg protracts and retracts. At its peak flexure, the tarsus bends 50 *degrees* to maintain the correct gripping force angle.

In Figure 17, forward body motion in two different orientations with respect to gravity is shown in subfigures (a) and (b) with a stationary turn shown in subfigure (c). These data were obtained through video analysis of DIGbot steps. Bright markers were attached to the fore and aft hip locations, and the motion of these points was tracked in post processing for a step.

Results for horizontal stepping on a vertical surface are shown in Figure 17a. The desired forward motion and the mean value of the measured steps are shown. During this motion, the vertical forces used to oppose gravity and maintain posture are mostly decoupled from the horizontal forces that generate the desired motion; the weight of DIGbot is not working against its progress. The motors achieve their desired position and result in accurate motion.

In Figure 17b, data are presented for eight forward steps up a vertical screen surface. More steps are shown here to provide a more complete picture of the typical performance. The forward motion does not reach the desired motion for several primary reasons: 1) steady state errors persist in the joint motors as they attempt to overcome the force of gravity, 2) occasionally during a step, a claw will shift from its initial screen gap to a different gap for which the control system is not designed to compensate, 3) the body frame and leg braces are flexible and result in differences between the desired and actual body motion when the system is loaded, and 4) the body is kept close to the screen to reduce the tipping moment, so the belly of DIGbot occasionally catches on surface asperities and inhibits the motion.

In Figure 17c, data are presented for a 33 *degree* stationary turn on a vertical screen. This motion results in a large deviation among the trials, which don't correlate well with the desired turn angle. All of the turns shown fall short of the desired turn. This is largely due to the claw getting pulled out of its original foothold and reattaching to in inward hole in the mesh screen. This occurs more often during turns than straight walking because the leg angle changes are large during a step, which results in large tarsus angle deflections. Despite the resulting errors, throughout all of the tests shown in Figure 17, the feet remain in contact with the surface and support DIGbot.

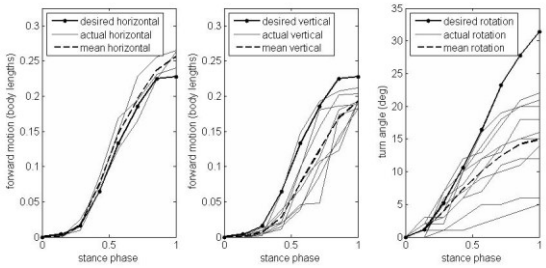

(a) (b) (c)

Figure 17. Body motion during forward steps and a stationary turn. The desired values are kinematically calculated and shown, along with the mean values from the trials shown. Subfigure (a) shows the motion during a forward step with the robot oriented horizontally on a vertical surface. The weight of the robot does not act against the motion and the actual motion approaches the desired motion. Subfigure (b) shows the motion during a forward step up a vertical surface. In this orientation, the weight of the robot works against the motion and causes the actual motion to fall short of the desired motion. Subfigure (c) shows the rotation of DIGbot during a turn in place on a vertical surface. Problems result from spine slipping, but the legs maintain adhesion with the surface.

Inward gripping forces during two representative steps are shown in Figure 18. The DIG threshold is set to 0.55 times body weight, which is only verified during the attachment phase. Once a foot is attached and its leg begins to retract, the inward force dips below this threshold value. DIGbot does not experience a failure when this occurs, as the DIG threshold is set adequately high to account for this variation in inward forces.

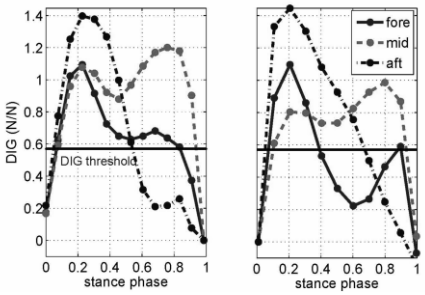

Figure 18. Inward gripping forces during two representative climbing steps. The DIG threshold is set to 0.55 times body weight, which is only verified during the attachment phase. It is expected that the DIG force may dip below the initial threshold during the stance phase, but no force feedback is required to prevent falling.

DIGbot failure rarely occurs while the body is moving. On occasion, the tip of the claw latches onto the raised intersection of the mesh wire, which keeps the claw from recessing into the mesh. The inward search process usually causes the tip to detach from this raised intersection and re-initiate the gripping process a previously described, but in rare cases, estimated by the authors as 5% of the walking steps, this does not occur and the DIG threshold force is achieved which falsely indicates an adequate foothold. When this leg assumes a significant portion of the body weight, after the other tripod detaches, the claw is pulled from this foothold. When walking inverted, the two remaining attached legs cannot support the load and the body falls from the screen. When climbing on a vertical surface, the body does not always fall from the screen. In some of these cases, the two remaining attached legs are able to hold the body onto the screen but the body is pitched away from the screen such that the contralateral leg of the other tripod cannot reach the screen with its preplanned trajectory for depression toward the screen. Future iterations of the DIG algorithm will include more corrective behaviors for these rare scenarios.

Feedback during stance was at one time used to maintain a constant DIG force during retraction. The gripping force was adjusted by moving the commanded foot position laterally inward or outward using proportional feedback from the servo torques, but was ultimately found not to improve the success of the algorithm. The data rate for the force feedback of the 18 motors used by the three supporting legs is 7 *Hz*. The body is only in motion for 0.5 *second* intervals, so only two reads of the leg force occured during each step. This did not allow for adequate correction of the leg position when the force drops below the threshold, so this strategy was ultimately abandoned.

Video of DIGbot can be viewed at http://www.cse.usf.edu/~palmer/climbing.htm.

VI. Discussion

This paper describes the implementation of Distributed Inward Gripping (DIG) as an attachment and adhesion strategy for gravity-independent climbing. DIG is a biologically-inspired approach that is used by insects and other small animals to climb up, under, over and onto surfaces of varying roughness, and in any orientation with respect to gravity. This attachment strategy relies on directional attachment mechanisms, which are characterized by their ability to support attachment forces normal to the surface when a shear force is applied in a particular direction. The normal attachment force is reduced to zero when the shear loading is relaxed, making detachment rapid and energetically inexpensive when compared to other attachment and detachment strategies.

The DIG attachment strategy is implemented on an 18-DOF hexapod that can walk and make turns on vertical and inverted surfaces. In nature, directional attachment mechanisms appear in the form of articulating digits, claws, spines and dry adhesive pads with directionally-oriented microscopic hairs. DIGbot employs a single claw on each foot to climb on mesh screen. The robot does a local search for a solid foothold around the initial foot touchdown position because the robot has no knowledge of where the claw is relative to the wire. With regular spacing in a wire mesh, the robot is guaranteed to find a foothold whereas on natural surfaces this is not certain. The algorithm can be adapted for more irregular surfaces by increasing the search space for a potential foothold. The presented foothold searching behavior is also relevant to robots using directional animal-inspired dry adhesive pads for attachment. Foot gripping must be obtained and tested in a similar manner.

This work is inspired by the impressive performance of climbing insects. Even a fraction of their mobility in any orientation with respect to gravity, combined with tele-operative capabilities in a legged system would prove useful for many applications such as planetary exploration, time-critical search and rescue and military reconnaissance. Distributed inward gripping was shown to be a viable attachment strategy for climbing, but further work needs to be accomplished. More can be learned about DIG during more complex maneuvers, such as transitioning between orthogonal surfaces and walking on more natural terrains. Figure 19 shows DIGbot climbing a tree and telephone pole with stiff claws in place of the compliant tarsi to achieve the required grip. The climbing algorithm can be developed further to allow for climbing a variety of surfaces using a single versatile foot.

Figure 19. DIGbot climbing on a tree trunk and telephone pole with stiff claws.

The system is currently too massive to climb smooth surfaces using available directional dry adhesives. Minimizing size was not an initial design goal for this project, but continued research into this attachment mechanism will lead to developments that can be implemented in a smaller system designed to employ dry adhesives in combination with claws as found in climbing animals.

Acknowledgements

The authors also gratefully acknowledge the contribution of Dr. Cindy Harley and Dr. Roy Ritzmann for use of their biology lab and for useful cockroach insight and videos.

Funding

This work was supported by the United States Intelligence Community Postdoctoral Fellowship and the Case Western Reserve University Office of Support for Undergraduate Research and Creative Endeavors.

References

- Asbeck, A. T., Kim, S., Cutkosky, M. R., Provancher, W. R , Lanzetta, M. (2006). “Scaling Hard Vertical Surfaces with Compliant Microspine Arrays. *International Journal of Robotics Research*, vol. 25(12):1165–1179.

- Autumn, K., Dittmore, A., Santos, D., Spenko, M. and Cutkosky, M. (2006). Frictional adhesion: a new angle on gecko attachment. *Journal of Experimental Biology*, vol. 209: 3569-3579.
- Autumn, K., Hsieh, S., Dudek, D., Chen, J., Chitaphan, C. and Full, R. (2006). Dynamics of geckos running vertically, *Journal of Experimantal Biology*, vol. 209: 260-272.
- Bassler, U. (1993). The walking- (and searching-) pattern generator of stick insects, a modular system composed of reflex chains and endogenous oscillators. *Biological Cybernetics*, vol. 69(4): 305-217.
- Bevly, D., Dubowsky, S. and Mavroidis, C. (2000). A simplified Cartesian-computed torque controller for highly geared systems and its application to an experimental climbing robot. ASME Journal of Dynamic Systems, Measurement, and Control, vol. 122(1):27–32.
- Bretl, T., Rock, S., Latombe, J., Kennedy, B. and Aghazarian, H. (2004). Free-climbing with a multi-use robot. *Proceedings of the International Symposium on Experimental Robotics,* Singapore, pp. 449-458.
- Choi, H., Park, J. and Kang, T. (2004). A self-contained wall climbing robot with closed link mechanism. *Journal of Mechanical Science and Technology*, vol. 18: 573-581.
- Daltorio, K., Wie, T., Horchler, A., Southard, L., Wile, G., Quinn, R., Gorb, S. and Ritzmann, R. (2009). Mini-WhegsTM Climbs Steep Surfaces Using Insect-Inspired Attachement Mechanisms. *International Journal of Robotics Research*, vol. 28(2): 285-302.
- Delcomyn, F. (1987). Motor activity during searching and walking movements of cockroach legs. *Journal of Experimental Biology*, vol. 133: 111-120.
- Frazier, S., Larsen, G., Neff, D., Quimby, L., Carney, R., DiCaprio, R. and Zill, S. (1999). Elasticity and movements of the cockroach tarsus in walking. *Journal of Comparative Physiology A,* vol. 185: 157-172.
- Goldman, D., Chen, T., Dudek, D. and Full, R. (2006). Dynamics of rapid vertical climbing in cockroaches reveals a template. *Journal of Experimental Biology,* vol. 209: 2990-3000.
- Gonzalez de Santos, P. ,Armada, M.A., and Jimenez, M.A. (2000). Ship building with ROWER. *IEEE Robotics and Automation Magazine*, vol. 7(4): 35–43.
- Gorb, S., Sinha, M., Peressadko, A., Daltorio, K. and Quinn, R. (2007). Insects did it first: a micropatterned adhesive tape for robotic applications. *Bioinspiration & Biomimetics*, vol. 2: 117-125.
- Jindrich, D. and Full, R. (1999). Many-legged maneuverability: dynamics of turning in hexapods. *The Journal of Experimental Biology*, vol. 202: 1603–1623.
- Kim, S., Spenko, M., Trujillo, S., Heyneman, B., Mattoli, V. and Cutkosky, M. (2007) April 10-14. Whole body adhesion: hierarchical, directional and distributed control of adhesive forces for a climbing robot. *IEEE Conference on Robotics and Automation*, Rome, Italy, pp. 1268-1273.
- Kim, S., Spenko, M., Trujillo, S., Heyneman, B., Santos, D. and Cutkosky, M. (2008). Smooth vertical surface climbing with directional adhesion. *IEEE Transactions on Robotics*, vol. 24: 65-74.
- Lee, J., Bush, B., Maboudian, R. and Fearing, R. (2009). Gecko-inspired combined lamellar and nanofibrillar array for adhesion on nonplanar surface. *Langmuir,* vol. 25 (21): 12449-12453.
- Lynch, G., Clark, J., Lin, P., and Koditschek, D. (2012). A bioinspired dynamical vertical climbing robot. *International Journal of Robotics Research*, vol. 31: 974-996..
- Madhani, A. and Dubowsky, S. (1997). The force workspace: A tool for the design and motion planning of multi-limb robotic systems. *ASME Journal of Mechanical Design*, vol. 119(2):218–224.
- Mirats Tur , J. M. and Garthwaite, W. 2010. “Robotic devices for water main in-pipe inspection: A survey,” *Journal of Field Robotics*, vol. 27 (4): 491 – 508.
- Murphy, M., Aksad, B. and Sitti, M. 2008. Gecko-inspired directional and controllable adhesion. *Small*, vol. 5: 170-175.
- Murphy, M. and Sitti, M. 2007. Waalbot: An Agile Small-Scale Wall-Climbing Robot Utilizing Dry Elastomer Adhesives. IEEE/ASME Transactions on Mechatronics, vol. 12 (3): 330-338.
- Nguyen, VD 1988. “Constructing Force- Closure Grasps,” *International Journal of Robotics Research*, vol. 7, no. 3, pp. 3-16.
- Niederegger, S. and Gorb, S. 2003. Tarsal movements in flies during leg attachment and detachment on a smooth substrate. *Journal of Insect Physiology*, vol.49, pp. 611-620.
- Palmer III, L., Diller, E. and Quinn, R. 2009. Design aspects of a climbing hexapod. *Proceedings of the International Conference on Climbing and Walking Robots*, Istanbul, Turkey, pp. 197-204.
- Pearson, K and Franklin, R. 1984. Characteristics of Leg Movements and Patterns of Coordination in Locusts Walking on Rough Terrain. *The International Journal of Robotics Research*, vol. 3, num. 2, pp. 101-112.
- Ponce, J. and Faverjon, B. 1995. "On computing three-finger force-closure grasps of polygonal objects," *IEEE Transactions on Robotics and Automation*, vol.11, no.6, pp.868-881.
- Spenko, M., Haynes, G., Saunder, J., Cutkosky, M., Rizzi, A., Full, R. and Koditschek, D. 2006. Biologically inspired climbing with a hexapedal robot, *Journal of Field Robotics*, vol. 25, pp. 223–242.
- Tavakoli , Mahmoud, Marques, Lino and de Almeida, Aníbal T. 2010, "Development of an industrial
- pipeline inspection robot", *Industrial Robot*, vol. 37, num. 3, pp. 309 — 322.
- Tryba, A. and Ritzmann, R. 2000. Multi-Joint Coordination During Walking and Foothold Searching in the *Blaberus* Cockroach. I. Kinematics and Electromyograms. *The Journal of Neurophysiology*, vol. 83, num. 6, pp. 3323-3336.
- Wei, T., Quinn, R. and Ritzmann, R. 2004. A clawar that benefits from abstracted cockroach locomotion principles. *The 7th International Conference on Climbing and Walking Robots.* Madrid, Spain, pp. 849-857.
- Zhang, G., Zhang, J., Zong, G., Wang, W. and Liu, R. 2006. Sky cleaner 3: a real pneumatic climbing robot for glass-wall cleaning. *IEEE Robotics & Automation Magazine*, vol. 13, pp. 32-41.